5052铝合金/镀锌钢涂粉CO_2激光熔钎焊工艺特性

樊 丁[1,2], 蒋 锴[1], 余淑荣[1,2], 张 健[1]
(1. 兰州理工大学 甘肃省有色金属新材料省部共建国家重点实验室, 兰州 730050;
2. 兰州理工大学 有色金属合金及加工教育部重点实验室, 兰州 730050)

摘 要: 以5052铝合金和热镀锌ST04Z钢为研究对象,采用预置涂粉CO_2激光搭接熔钎焊方法进行工艺试验. 利用光学显微镜、扫描电镜和拉伸试验机对熔钎焊接头的微观组织和力学性能进行了研究. 结果表明,涂助溶剂和粉末后,焊缝成形明显改善,镀锌层没有烧损;熔—钎焊接头过渡层最大厚度小于10 μm,针状Al-Fe金属间化合物没有向熔化的铝侧明显析出;接头具有较高的力学性能,最大机械抗载能力可达到208 MPa,约为5052铝合金母材抗拉强度的95.41%.

关键词: 铝钢; 激光焊接; 熔钎焊; 粉末
中图分类号: TG456.7 **文献标识码:** A **文章编号:** 0253-360X(2014)01-0001-04

0 序 言

将钢与铝或铝合金连接成为异种金属结构,能充分发挥两种材料的性能优势,实现轻量化,在航空、船舶、石油化工和车辆制造工业中具有独特的优势和应用前景. 铝和钢两种金属物理化学上的巨大差异采用热熔焊方法很难实现连接[1]. 激光具有能量密度高、热量集中、热影响区小、焊接变形小等优点,可实现铝/钢异种金属优质高效连接.

铝/钢异种金属熔钎焊焊接过程中,熔化的液态铝在钢侧有效润湿铺展,如何减少脆硬的金属间化合物层的厚度,而获得优质高性能的焊接接头,成为近些年来研究的热点课题[2-6]. 文中在铝/钢激光搭接熔钎焊中,采用在铝板上预置涂粉方法,可显著提高激光吸收率,很大程度上提高了焊接速度,抑制了Al-Fe金属间化合物的形成,也使液态铝易于在钢侧有效铺展. 最后通过优化工艺,获得了成型良好,力学性能较高的铝钢熔钎焊接头.

1 试验方法

试验中采用的5052铝板和ST04Z镀锌钢板的尺寸为150 mm×70 mm×1.0 mm,5052铝合金材料的化学成分如表1所示. ST04Z镀锌钢的化学成分如表2所示.

表1 5052铝合金的化学成分(质量分数,%)
Table 1 Chemical compositions of 5052 aluminum alloy

Si	Mn	Mg	Cu	Fe	Cr	Zn	Al
0.25	0.10	2.35	0.10	0.40	0.20	0.10	余量

表2 ST04Z镀锌钢的化学成分(质量分数,%)
Table 2 Chemical compositions of ST04Z stainless steel

C	Mn	Si	P	S	Cu	Zn	Ni
0.08	0.4	≤0.40	0.02	≤0.30	≤0.15	≤0.15	≤0.15

试验所用的激光为GS-TFL-10KCO_2高功率横流CO_2激光器,主要技术指标:波长为10.6 μm;不稳定性≤3%;气体成分为CO_2:N_2:He=1:10:20;电源380 V±10%、频率50 Hz、电流120 W;额定激光功率≥10.0 kW;焊接模式为多模.

试验前对5052铝合金板用机械和化学清理方法去掉表面的氧化膜,用丙酮去掉镀锌钢板表面的油污. 表面处理干净的板材组合成搭接接头(铝板在上,镀锌钢板在下),焊接过程中首先在助熔剂中加入溶剂(丙酮)涂敷在铝合金焊道表面,待丙酮蒸发后,将混合均匀的粉末加入溶剂(丙酮)搅拌均匀涂敷在已涂助熔剂的焊道表面,涂敷厚度以遮盖铝合金表面为宜. 粉末成分如表3所示.

表3 粉末成分(质量分数,%)
Table 3 Chemical compositions of metal powder

Si	Mn	Mg	B	Zn	Al
1~3	1~3	5~8	0.5~1	5~10	余量

收稿日期: 2012-11-30
基金项目: 甘肃省自然科学基金资助项目(3ZS041-A25-031)

对试样做拉伸性能试验，拉伸速度为 1 mm/min，用 JSM-6700F 扫描电镜观测断口形貌特征，制取金相试样，用 100 mL 蒸馏水、5mL HNO_3，2 mL HCl 和 2 mL HF 配置的混合酸腐蚀金相试样铝合金侧，对金相试样做组织分析和硬度试验.

2 试验结果和讨论

2.1 铝钢激光熔钎焊焊缝成形特点

铝钢异种金属搭接熔钎焊(铝在上钢在下)，不涂粉末和助熔剂时很难焊接. 如图 1 所示，不涂助溶剂仅涂粉末时焊缝成形不连续或焊不上，焊缝靠铝板侧发皱且有微量飞溅; 涂助溶剂后焊缝成型良好，焊缝靠铝板侧没有发皱现象，且无飞溅. 由于助溶剂能有效去除焊前没有清理完全或在焊接之前这段时间内产生的氧化膜，而氧化膜不易熔化，粉末熔化后在其上易产生飞溅，且加热冷却时发生收缩起皱. 当激光功率为 2.1 kW，焊接速度为 0.6 m/min 时，涂助溶剂和粉末得到的焊缝形貌如图 2 所示，可以看出焊缝成形良好，背面热影响区很小，镀锌层没有烧损. 图 3 为铝钢熔钎焊接头截面形貌.

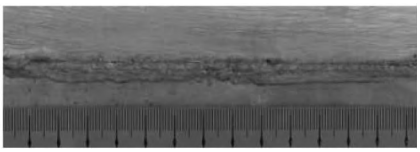

图 1 涂粉末不涂助熔剂时焊缝形貌

Fig. 1 Weld appearance with metal powder without flux

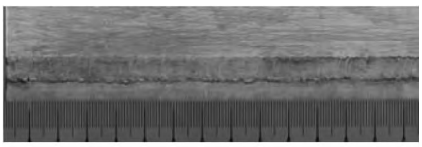

(a) 焊缝正面

(b) 焊缝背面

图 2 涂助溶剂和粉末时焊缝形貌

Fig. 2 Weld appearance with powder and flux

试验得到的合适的焊接工艺参数是: 激光功率 1 500 ~ 2 500 W，焊接速度 0.4 ~ 1.2 m/min，离焦量 −2 ~ +2 mm.

2.2 微观组织特征

图 4、5 为焊缝熔合区金相照片和 SEM 形貌，从

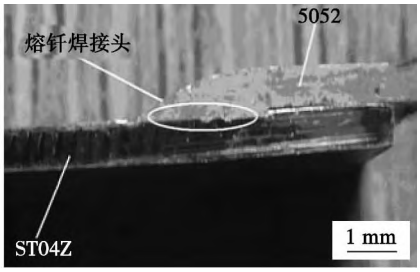

图 3 铝钢激光熔钎焊接头截面形貌

Fig. 3 Sectional view of laser fusion-brazing joint

图中可以看出镀锌钢未熔化，而且 5052 铝合金与镀锌钢之间有一层过渡层，这主要是由铝母材和粉末熔化后向镀锌钢侧扩散而形成的典型的熔—钎焊接头. 在冷却速度较快的条件下过渡层最大厚度小于 10 μm，没有发现明显的针状 Al-Fe 金属间化合物向铝侧析出. 熔化区内由于冷却速度快，二次相不易析出，枝晶网不连续，从靠近过渡层到熔化区边缘，依次出现柱状晶和等轴晶.

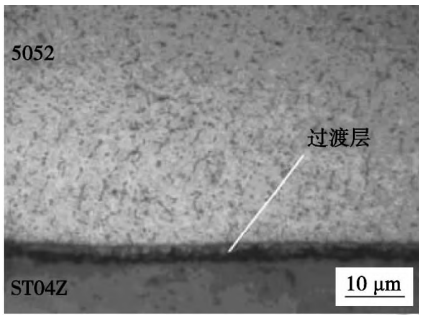

图 4 焊缝熔合区金相形貌

Fig. 4 Metallograph of fusion-brazing joint zone

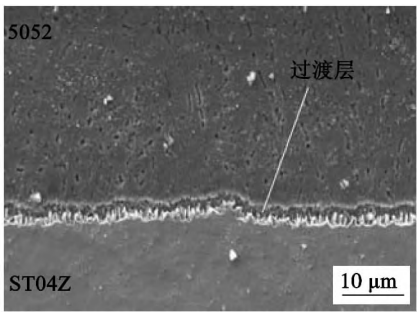

图 5 焊缝熔合区 SEM 形貌

Fig. 5 SEM of fusion-brazing joint zone

2.3 焊缝的力学性能

对 5052 铝合金和镀锌钢的激光熔—钎焊接头进行拉伸试验，图 6 为铝钢激光熔—钎焊接头的拉伸断裂形貌，图 7 为铝钢激光熔钎焊接头和铝母材的应力—应变曲线. 熔—钎焊接头拉伸试样断裂的

位置在 5052 铝合金母材,具有较高的机械抗力,最大机械抗力可达到 208 MPa,约为 5052 铝合金母材抗拉强度的 95.41%(实测 5052 铝合金的平均抗拉强度为 218 MPa);部分试件在热影响区或焊缝处断裂,平均机械抗力达到 185 MPa,约为母材的 84.9%. 由于搭接接头还受到剪切力的作用,拉伸断裂后钢板钎焊部位均有向背面 10°~30°弯曲. 在文献[7-9]中,铝钢熔钎焊接头的力学性能最大能达到 155 N/mm,相比较而言文中试验所得到的激光熔钎焊接头力学性能更高.

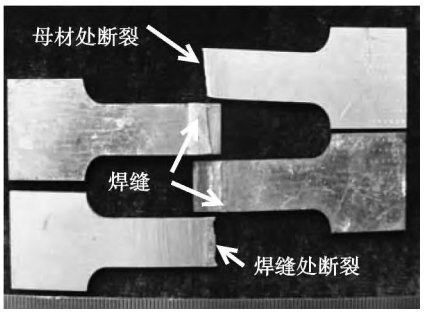

图 6　铝钢激光熔钎焊接头拉伸断裂形貌

Fig. 6　Tensile fracture specimens of laser fusion-brazing joint

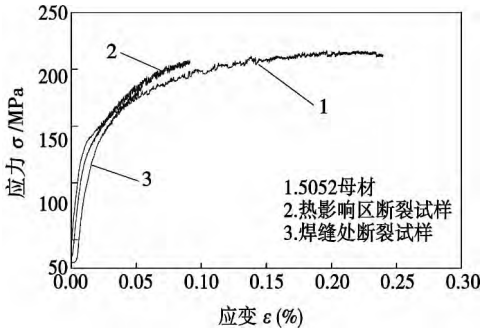

图 7　试样和母材应力—应变曲线

Fig. 7　Stress-strain curve specimens and 5052 aluminum alloy

对焊缝处断裂的铝钢熔—钎焊接头进行断口扫描,断口形貌的 SEM 形貌如图 8 所示. 可以看出靠近镀锌钢侧断口主要是解理组织,而远离镀锌钢侧主要是小韧窝断裂,主要由于拉伸后搭接接头受到剪切力发生弯曲后从钎焊区部分被撕裂,撕裂的正好发生在脆性的过渡层(Al-Fe 金属间化合物层),所以靠近镀锌钢侧断口主要为脆性断裂.

为了进一步分析过渡层的强度,对金相试样给予适当的剪切力,用金相显微镜观察断裂特征,如图 9 所示,断裂面在熔化的铝侧而不是在过渡层,这

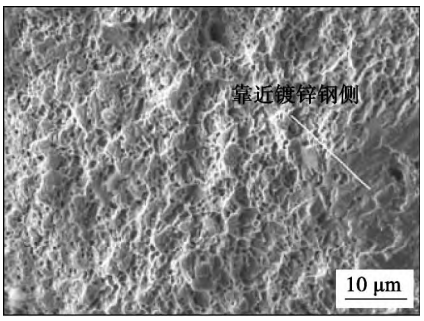

图 8　接头拉伸断口形貌(焊缝处断裂)

Fig. 8　SEM micrograph of fracture surface

说明裂纹不是由脆硬的过渡层(Al-Fe 金属间化合物)引起的,接头更能够满足力学性能要求.

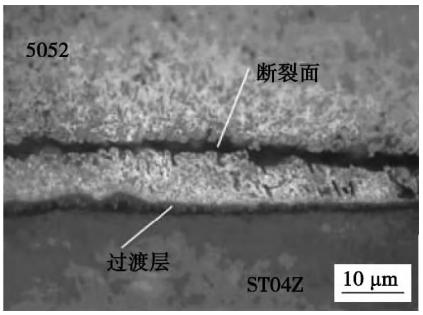

图 9　断裂面金相形貌

Fig. 9　Metallograph of crack

对铝钢激光填粉熔钎焊进行显微硬度试验,如图 10,图 11 所示,过渡层硬度明显高于熔化层和钢侧,最大硬度值达到 8 467 MPa(Al-Fe 金属间化合物的硬度为: Fe_2Al_5 ~9 927 MPa, $FeAl_3$ ~8 742 MPa, $FeAl_2$ ~10 388 MPa, FeAl ~4 606 MPa, Fe_3Al ~3 430 MPa[10]),熔化层和靠近过渡层钢侧硬度高于铝合金和镀锌钢母材,这主要是由于粉末中的硅、锰、镁等形成强化相,同时快速加热和冷却对镀锌钢进行了淬火,导致其硬度高于母材(铁的硬度为 2 156 ~ 2 352 MPa,铝的硬度为 1 323 ~1 421 MPa).

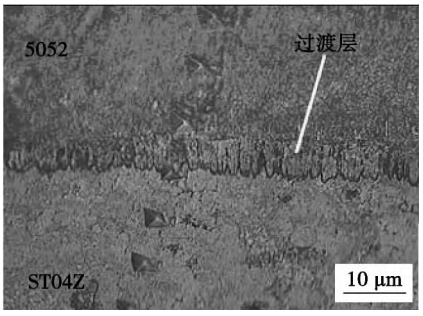

图 10　接头显微硬度金相形貌

Fig. 10　Metallograph of micro-hardness

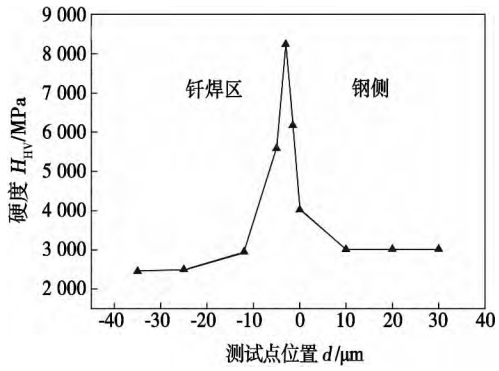

图11 试样接头的显微硬度

Fig. 11 Micro-hardness of fusion-brazing joint

3 结 论

(1) 涂助溶剂和粉末后激光吸收率显著提高，焊缝成形良好，焊缝靠铝板侧没有发皱现象，且无飞溅；背面热影响区很小，镀锌层没有烧损. 试验得到的合适的工艺参数是：激光功率1 500～2 500 W，焊接速度0.4～1.2 m/min，离焦量－2～＋2 mm.

(2) 激光熔钎焊接头过渡层最大厚度小于10 μm，没有发现针状Al-Fe金属间化合物明显向熔化的铝侧析出；从靠近过渡层到熔化区边缘，依次出现柱状晶和等轴晶.

(3) 激光熔钎焊接头具有较高的力学性能，最大机械抗力可达到208 MPa，约为5052铝合金母材抗拉强度的95.41%. 焊缝处断裂的铝钢熔—钎焊接头主要是小韧窝断裂，靠近镀锌钢侧有解理组织.

参考文献：

[1] Ishida T. Interfacialphenomena of plasma arc welding of mild steel and aluminium [J]. Journal of Materials Science, 1987, 22: 1061－1066.

[2] Ka Wakatsu, Osawa T. Furnacebrazing of steel with brass filler metal [J]. Welding Journal, 1977, 56(2): 56～60.

[3] Roulin M, Luster J W, Karadenz G. Strength and structure of furnace-brazed joints between aluminum and stainless steel [J]. Welding Journal. 1999, 78(5): 151－155.

[4] Murakami T, Nakata K, Honjun Tong. Dissimilar metal joining of aluminum to steel by MIG arc brazing using flux cored wire [J]. ISIJ International, 2003, 43(10): 1596－1602.

[5] Nishimoto K, Fujii H, Katayama S. Laser pressure welding of Al alloy and low C steel [J]. Science and Technology of Welding and Joining, 2006, 11(2): 224－231.

[6] Honggang Dong, Weijin Hu. Dissimilar metaljoining of aluminum alloy to galvanized steel with Al-Si, Al-Cu, Al-Si-Cu and Zn-Al filler wires [J]. Journal of Materials Processing Technology, 2012, 212: 458－464

[7] 雷 振，于 宁. 5A02/Q235钢Nb：YAG激光－脉冲MIG复合热源熔－钎焊 [J]. 焊接学报，2008，29(6)：21－24
Lei Zhen, Yu Ling. Fusion-brazing joining between 5A02 aluminium alloy and Q235 steel by Nd: YAG laser-pulsed MIG hybrid welding [J]. Transactions of the China Welding Institution, 2008, 29(6): 21－24.

[8] 石 岩，张 宏，渡部武弘，等. 连续－脉冲双激光束焊接钢－铝合金 [J]. 中国激光，2010，37(4)：1132－1137.
Shi Yan, Zhang H ong, Takehiro Watanabe, *et al*. CW/ PW dual-beam YAG laser welding of steel/ aluminun alloy sheets [J]. Chinese Journal. Laser, 2010, 37(4): 1132－1137.

[9] 张冬云，高双欣. 铝/钢异种金属激光填丝熔－钎焊连接工艺研究 [J]. 激光与电子学进展，2011，48(6)：1－8.
Zhang Dongyun, Gao Shuangxin. Wire feeding laser brazing and fusion for Al-Fe dissimilar metal [J]. Laser & Optoelectronics Progress, 2011, 48(6): 1－8.

[10] Rathod M J, Katsuna M. Joining of aluminum alloy 5052 and low-carbon steel by laser roll welding [J]. Welding Journal, 2004, 83(1): 16－26.

作者简介： 樊 丁，男，1961年出生，教授，博士研究生导师. 主要从事焊接物理、焊接方法与智能控制及激光加工等方面的研究. 发表论文200余篇. Email: fand@lut.cn

MAIN TOPICS, ABSTRACTS & KEY WORDS

Characteristic of fusion-brazed joint between 5052 aluminum alloy and zinc-coated steel by CO_2 laser FAN Ding[1,2], JIANG Kai[1], YU Shurong[1,2], ZHANG Jian[1] (1. State Key Laboratory of Gansu Advanced Non-ferrous Metal Materials, Lanzhou University of Technology, Lanzhou 730050, China; 2. Key Laboratory of Non-ferrous Metal Alloys and Processing of Ministry of Education, Lanzhou University of Technology, Lanzhou 730050, China). pp 1 - 4

Abstract: Welding between aluminum and steel has become a hot and difficult problem in the field of welding. By means of CO_2 laser welding and brushing metal powder and flux before welding, overlap fusion-brazed joint between 5052 aluminum alloy and ST04Z zinc-coated steel sheets was obtained, in which the 5052 aluminum alloy was melted but zinc-coated sheet was brazed. The microstructure in the joint and fracture features of the tensile specimen were investigated by optical microscope, scanning electron microscope (SEM) and universal testing machine. The results indicate that after brushing metal powder and flux, the laser absorption could be improved greatly, and the resultant weld appearance was sound and the zinc-coated layer was not burned. The thickness of the intermediate layer was less than 10 μm, and acicular intermetallic compounds did not diffuse into the aluminum weld. The maximum tensile strength of the joint was 208 MPa, about 95% of 5052 aluminum alloy.

Key words: aluminum alloy and steel; laser welding; fusion-brazing; metal powder

Characteristics of welding arc during ultrasound-MIG hybrid welding of aluminum alloy FAN Chenglei[1], XIE Weifeng[1], YANG Chunli[1], KOU Yi[2] (1. State Key Laboratory of Advanced Welding and Joining, Harbin Institute of Technology, Harbin 150001, China; 2. Changchun Faw-Volkswagen Automotive Co., Ltd, Changchun 130011, China). pp 5 - 8

Abstract: In order to better understand the ultrasound-MIG welding process, the arc behavior during ultrasonic-MIG welding of aluminum alloy was investigated in this paper. The response of ultrasound-arc was explored at different wire feeding speeds or welding voltages. The results show that the compression effects of ultrasound-arc varied with different welding parameters. With the increase of wire feeding speed, the compression gradually became weaker. According to the results, the analysis of ultrasound-arc self-adjusting was carried out. Compared with the traditional MIG welding, the electric field strength and temperature in ultrasonic arc were greatly enhanced and led to stronger welding stability.

Key words: arc compression; electric field intensity; particle motion; temperature field; self-regulation

Microstructure and shear strength of high-temperature brazed joint of Super-Ni/NiCr laminated composite using Ni-Cr-Si-B filler metal WU Na, LI Yajiang, WANG Juan (Key Laboratory for Liquid-Solid Structural Evolution and Processing of Materials (Ministry of Education), Shandong University, Jinan 250061, China). pp 9 - 12, 36

Abstract: Super-Ni/NiCr laminated composite and Cr18-Ni8 steel were brazed with Ni-Cr-Si-B high-temperature brazing filler metal. The microstructure, phase constitution, shear strength and fracture morphology were analyzed. The brazed region consisted of γ-Ni solid solution, Ni_3B, CrB and Ni_3Si. The microhardness fluctuated across the brazed region. The microhardness of γ-Ni substrate was 450 MPa and that of Ni_3B was 650 MPa. The shear strength of the joint increased to 158 MPa as the brazing temperature increased to 1 120 ℃. The fracture surface displayed brittle features with some shearing dimples. Ni_3B interface formed between the super-Ni and brazed region. The joint fractured through the Ni_3B interface.

Key words: laminated composite; high-temperature brazing; microstructure; shear strength

Interface microstructure and mechanism of SiC ceramic vacuum brazed joint FENG Guangjie[1], LI Zhuoran[1], Xu Kai[1], LIU Wenbo[2] (1. State Key Laboratory of Advanced Welding and Joining, Harbin Institute of Technology, Harbin 150001, China; 2. AVIC Harbin Dongan Engine Co., Ltd, Harbin 150066, China). pp 13 - 16

Abstract: Vacuum brazing of SiC ceramic was conducted using Ti-Zr-Ni-Cu solder. The interface microstructure and its formation mechanism was investigated. Scanning electron microscope (SEM) was used to observe the joint microstructure and conduct local energy spectrum analysis. The results show that the products in the joint interface were mainly TiC, Ti_5Si_3, Zr_2Si, Zr(s,s), Ti(s,s) + Ti_2(Cu, Ni) and (Ti,Zr)(Ni,Cu) phases. The microstructure of the joint interface could be expressed as SiC/TiC/Ti_5Si_3 + Zr2Si/Zr(s, s)/Ti(s, s) + Ti_2(Cu,Ni)/(Ti,Zr)(Ni,Cu). The brazing process could be divided into five stages: physical contact between the solder and substrate, melting of solder and formation of reaction layer on the ceramic side, continuous diffusion of melted solder into the substrate, thickness increasing of reaction layer, composition homogenization, ending of reaction on ceramic side and formation of hypereutectic structure, solidification of intermetallic compounds in the center of joint. The shear strength of the joint brazed at 960 ℃ for 10min reached 110 MPa.

Key words: ceramic; vacuum brazing; microstructure; mechanism

Analysis of improving stability of welding technology by applying auxiliary electric field between slag and metal LI Xiaoquan, YANG Zonghui, ZHAO Zhiguo (School of Material Engineering, Nanjing Institute of Technology, Nanjing 211167,